

Synthesis and characterization of carboxymethylated cyclosophoraose, and its inclusion complexation behavior

Sanghoo Lee, Heylin Park, Donghyuk Seo, Youngjin Choi and Seunho Jung*

Department of Microbial Engineering and Bio/Molecular Informatics Center, Konkuk University, 1 Hwayang-dong, Gwangjin-gu, Seoul 143-701, South Korea

Received 21 July 2003; accepted 13 November 2003

Abstract—Carboxymethylated cyclosophoraoses (CM-Cys) were synthesized by chemical modification of a family of neutral cyclosophoraoses isolated from *Rhizobium leguminosarum* biovar *trifolii*. Structural analyses of the CM-Cys were carried out using NMR and FTIR spectroscopies, and the molecular weight distributions were confirmed with MALDI-TOF mass spectrometry. Based on structural characterization, native cyclosophoraoses were successfully substituted with carboxymethyl groups at the OH-4 and OH-6 of the glucose residues with degrees of substitution (DS) ranging from 0.012 to 0.290. CM-Cys was also used as a host for the inclusion complexation with hydrobenzoin (HB) and *N*-acetyltryptophan (*N*-AcTrp) as guest molecules. NMR spectroscopic analyses of the complexes showed that the CM-Cys induced chemical shifts of some protons of the guest molecules upon the complexation. Phase solubility studies of the guest molecules by CM-Cys were performed using HPLC, and the results were compared with those of native cyclosophoraoses. The solubility of HB and *N*-AcTrp was enhanced by the CM-Cys about 5.1- and 299-fold, respectively.

© 2003 Elsevier Ltd. All rights reserved.

Keywords: Carboxymethylated cyclosophoraoses; Chemical modification; *Rhizobium leguminosarum* biovar *trifolii*; Structural analyses; Inclusion complex; Hydrobenzoin; *N*-Acetyltryptophane

1. Introduction

Cyclosophoraoses are a class of unbranched cyclic oligosaccharides composed of β -(1 \rightarrow 2)-D-glucans varying in size from 17 to 40 as a neutral or anionic form.¹ Cyclosophoraoses play an important role in regulation the osmolarity in response to external osmotic shock² as well as on the successful root-nodule formation of *Rhizobium* species at the initial stage of nitrogen fixation.^{3–5} For the application of inclusion complexation, a single cyclosophoraose consisting of DP 17 (Cys-A) had been used as a host molecule.⁶ However, the isolated Cys-A showed a limited complex-forming ability over various hydrophobic guest molecules. Recently, many studies have been focused on the complexation of a family of

cyclosophoraoses with poorly soluble compounds such as ergosterol, indomethacin, paclitaxel, and luteolin.^{7a–d} In addition, the recognition of chirality by neutral and anionic cyclosophoraoses has recently been reported.⁸ Although their exact three-dimensional structures are not clearly known, NMR⁹ and conformational analyses¹⁰ have indicated that cyclosophoraoses seem to have flexible backbone structures and narrower cavity sizes than those expected from their bulky ring sizes.

To further applications of cyclosophoraoses, it is possible to modify their functional hydroxyl groups with a specific substituent through chemical derivatization. In this study, native cyclosophoraoses were modified with carboxymethyl groups through chemical derivatization, and their modified structures were investigated with nuclear magnetic resonance (NMR) and Fourier transform infrared (FTIR) spectroscopy and by matrix-assisted laser desorption/ionization-time of flight (MALDI-TOF) mass spectrometry. Finally, inclusion

* Corresponding author. Tel.: +82-2-450-3520; fax: +82-2-452-3611; e-mail: shjung@konkuk.ac.kr

complexation of the CM-Cys was performed with hydrobenzoin (HB) or *N*-acetyltryptophan (*N*-AcTrp) as guest molecule. The complex formation was investigated by ^1H NMR experiment and the concentrations of complexes was then quantitatively determined with high-performance liquid chromatography (HPLC).

2. Results and discussion

2.1. Isolation and identification of neutral cyclosophoraoses from *R. leguminosarum* bv. *trifolii*

Isolation, purification, and structural analyses of neutral cyclosophoraoses were carried out as described previously.⁷ Purified native cyclosophoraoses were separated with a R_f value of 0.125 on TLC. Ring sizes of native cyclosophoraoses, ranging from DP 17 to 26 (data not shown), were confirmed through MALDI-TOF mass spectrometry.

2.2. Synthesis, structural analysis, and molecular modeling study of CM-Cys

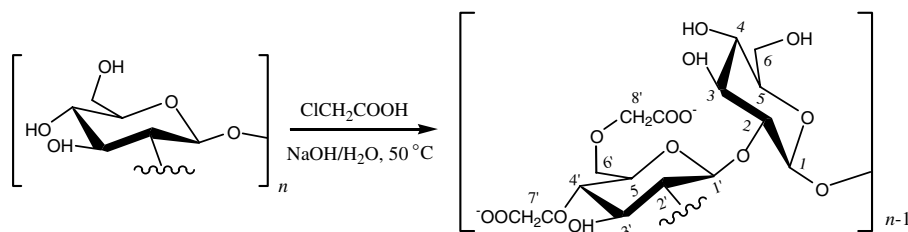
The hydroxyl groups of native cyclosophoraoses were subjected to chemical modification with ClCH_2COOH . The reaction was monitored on TLC. The R_f value of the purified CM-Cys was 0.285. The CM-Cys was synthesized in an 85% yield by a one-step process (Scheme 1).

The structure of CM-Cys was characterized with NMR and FTIR spectroscopy and by MALDI-TOF MS. In the ^{13}C NMR spectrum, each resonance of C-1 to C-6 carbons of CM-Cys was assigned at 102.4, 82.6, 75.8, 69.2, 76.7, and 61.1 ppm, respectively (Fig. 1a and b). Five peaks were also newly observed and assigned to the carbonyl carbons ($\text{C}=\text{O}$) of the carboxymethyl substituents at 178 ppm. The substituted C-4' carbon was assigned at 78.5 ppm, and the methylene carbons ($-\text{CH}_2-$) appeared at 69.9, 70.5, and 71.3 ppm. The methylene carbons at 69.9, 70.5, and 71.3 ppm were assigned to the C-6 carbons of the substituted glucopyranose units, the C-7' and C-8' carbons of the carboxymethyl groups are substituted at positions 6 and 4, respectively, as shown in

Scheme 1. In the HSQC spectrum, the signal of H-4' proton at 3.53 ppm, which overlapped with the H-4 proton of unsubstituted glucopyranose units, was correlated with the corresponding carbon signal. The signals of the H-6'a, H-6'b, H-7', and H-8' protons at 3.92, 3.83, 4.25, and 4.09 ppm, respectively, were also correlated with the corresponding carbon signals (Fig. 2). The substitution patterns were further confirmed with COSY and HMBC spectra. In HMBC spectra, long-range couplings were observed between the methylene carbons and the methylene protons substituted at positions 4 and 6. However, no substituent was observed at position 3 of the glucopyranose units (data not shown). Thus, these results indicated that native cyclosophoraoses were predominantly substituted with carboxymethyl groups at positions 4 and 6.

Figure 3 shows the FTIR spectra of native cyclosophoraoses (upper trace) and CM-Cys (lower trace). In the spectrum of CM-Cys, the C–O stretching band at 1074 cm^{-1} corresponding to the hydroxyl groups of the native cyclosophoraoses was significantly weakened, indicating that the carboxymethyl groups were successfully substituted at the hydroxyl positions. The O–H stretching band between 3600 and 3200 cm^{-1} was also very broad in the spectrum of CM-Cys. This could be explained as hydrogen-bonded hydroxyl groups of native cyclosophoraoses were predominantly associated with the substitution reaction. The asymmetric and symmetric stretching modes of the carboxylate groups ($-\text{COO}^-$) were observed as two absorption bands at 1598 and 1415 cm^{-1} , respectively. These stretching modes were typically observed in spectra of carboxymethylated polysaccharides.^{13,14}

Table 1 shows the measured and calculated mass data analyzed by MALDI-TOF mass spectrometry in the positive-ion mode. The measured mass units showed that the CM-Cys was acidic cyclosophoraoses with DS values ranging from 0.012 to 0.290. For CM-Cys of DP 21 with DS values ranging from 0.063 to 0.095 major mass peaks were observed corresponding to the differences between measured and calculated masses ranging from 24 to 28 Da. It indicates the presence of $[\text{M}+\text{Na}^++\text{H}^+]$, $[\text{M}+\text{Na}^++2\text{H}^+]$, $[\text{M}+\text{Na}^++3\text{H}^+]$, $[\text{M}+\text{Na}^++4\text{H}^+]$, and $[\text{M}+\text{Na}^++5\text{H}^+]$. For example, the CM-



Scheme 1. One-step synthesis of CM-Cys. The product shows the numbered β -(1 \rightarrow 2)-linked glucopyranose unit of carboxymethylated cyclosophoraoses. ($n = 17$ –26).

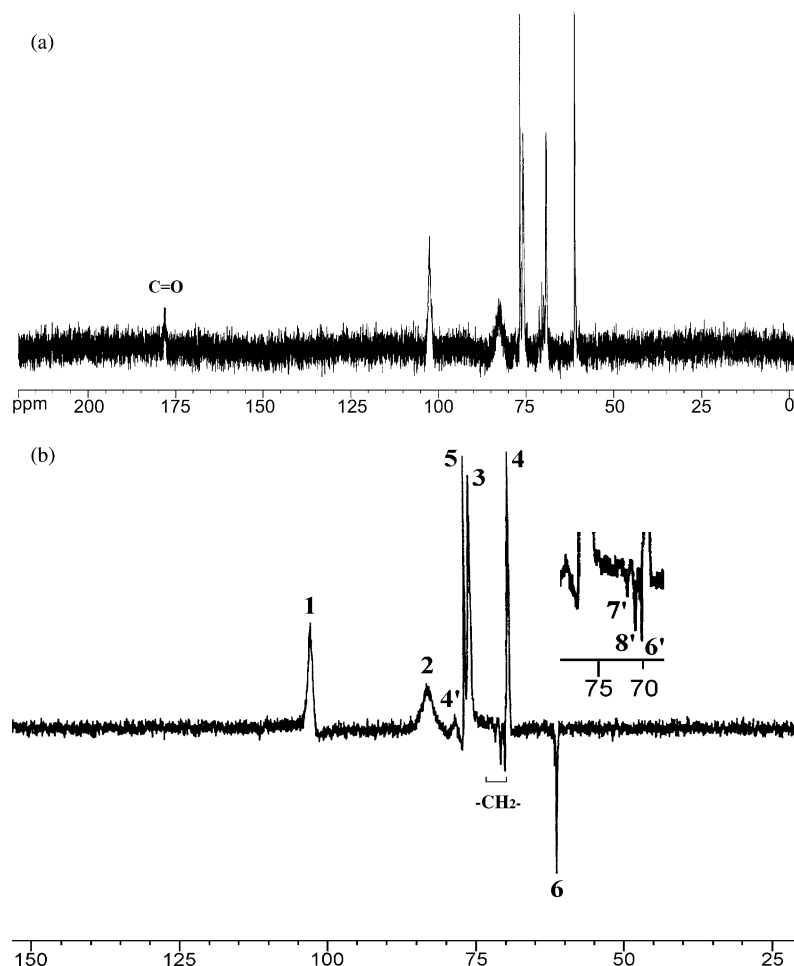


Figure 1. (a) ^{13}C NMR spectrum and (b) DEPT NMR spectrum of CM-Cys.

Cys of DP 22 with DS of 0.015 was observed as a measured value at m/z 3649, indicating the presence of $[\text{M}+\text{Na}^++4\text{H}^+]$. Molecular ion (M) indicates the molecular weight of the carboxymethylated cyclodextrin in the salt-free state. These multiple mass shifts have often been observed in mass patterns of acidic oligosaccharides.¹⁵ In addition, it was observed that the DS of CM-Cys decreased as the DP of CM-Cys increased.

Snapshots of CM-Cys21 (CM-Cys of DP 21) were obtained using a simulated annealing molecular dynamics (SA-MD) simulations (Fig. 4). The proposed model for CM-Cys21 (Fig. 4b) showed that it could have a different conformation from native cyclodextrins ($R_G = 8.5 \text{ \AA}$) (Fig. 4a).¹⁰ The average R_G (radius of gyration) value during the MD simulations in the presence of water became to be 9.2 \AA , where the increased R_G value would be due to the enhanced electrostatic repulsive interactions between the carboxyl groups of CM-Cys21. This conformational change could be responsible for the improved inclusion complex-forming ability of CM-Cys compared with native Cys.

2.3. Phase solubility studies of the complexes

Figure 5a shows the phase solubility diagrams of the complexed-HB with cyclodextrins and CM-Cys at 30°C . In the case of the CM-Cys-HB complex, the solubility diagram was the A_M type¹⁶ for which the initial slope is rising, followed by a plateau region, while, in the cyclodextrins-HB complex, the diagram was of the B_S type,¹⁶ in which the slope is rising in the initial stage and then is slightly decreased due to microcrystalline complex precipitation.¹⁷ Each solubility of HB and *N*-AcTrp was finally enhanced by CM-Cys about 5.1- and 299-fold, respectively (Fig. 5b).

2.4. ^1H NMR spectroscopic analysis of the inclusion complexes

^1H NMR experiments were performed to measure chemical shifts of both the host and guest molecules upon complexation. The chemical shifts were obtained for the complexes of 10 mM guests with 20 mM host molecules in D_2O at 25°C . Chemical shift variations in

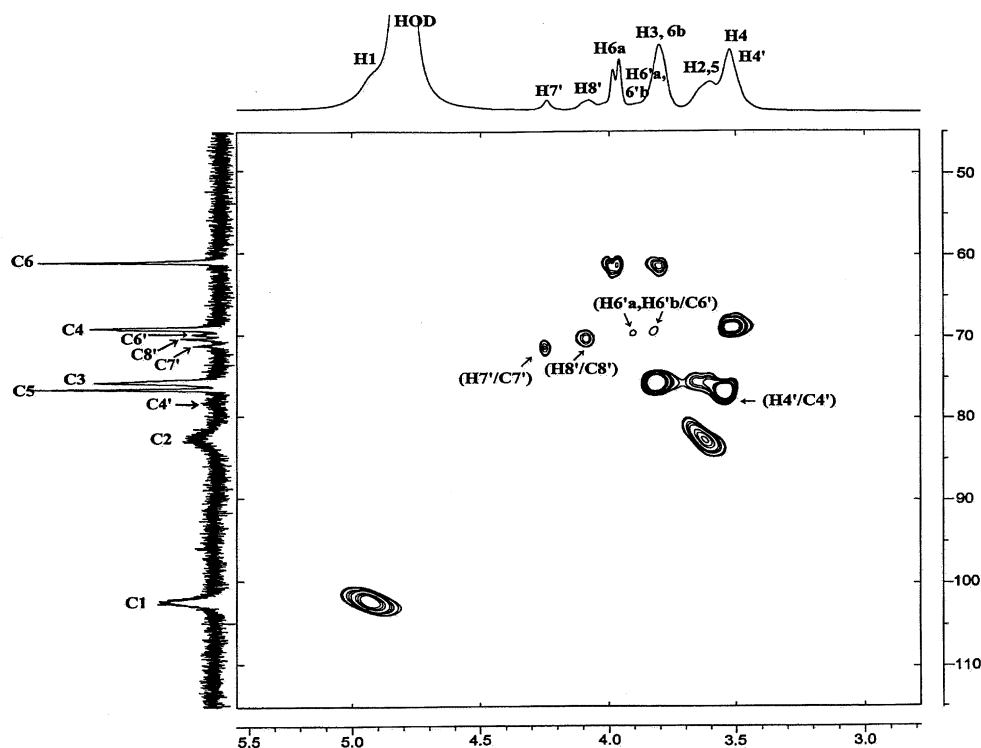


Figure 2. HSQC spectrum of CM-Cys. In this spectrum, the peak corresponding to the carbonyl carbon is not shown.

all the HB protons were observed upon the complexation with CM-Cys and cyclosophoraoses (Fig. 6a). The chemical shift was more pronounced on the H-7 proton of HB than the other protons. The H-7 proton of HB was shifted downfield, and the ring protons, H-2, -3, -4, -5, and -6, were shifted upfield, indicating that the protons of HB were surrounded by electron density of CM-Cys and cyclosophoraoses upon complexation. The magnitude of the shift of ring protons induced by CM-Cys was slightly larger than that by cyclosophoraoses. In the case of *N*-AcTrp, all the protons were shifted

upfield, except for H-9 and H-12, upon the complexation with CM-Cys and cyclosophoraoses. Especially, the H-2 and H-5 protons of *N*-AcTrp experienced significant chemical shifts. This indicates a stronger interaction of CM-Cys and cyclosophoraoses with the aliphatic region than with the ring moiety of *N*-AcTrp (Fig. 6b). The magnitude of the shifts induced by CM-Cys was larger than that by native cyclosophoraoses. Chemical shifts of the protons of CM-Cys and native cyclosophoraoses were also obtained upon the complexation with HB and *N*-AcTrp (Fig. 5c and d). The H-1 and H-2 protons of CM-Cys experienced noticeable chemical shifts upon complexation with HB and *N*-AcTrp, probably due to anisotropic effects of the magnetic field induced by the ring moieties of HB and *N*-AcTrp. Especially, this effect was clearly observed upon complexation with HB (Fig. 6c). It suggested that the H-1 and H-2 protons of CM-Cys associated with β -1,2-glycosidic linkages directly participated in the complexation with HB and *N*-AcTrp.

In this study, we investigated the synthesis of CM-Cys substituted with carboxymethyl groups from the isolated neutral cyclosophoraoses through a one-step chemical modification and its application for inclusion complexation. CM-Cys was confirmed to have DS values ranging from 0.012 to 0.290. NMR and FTIR spectroscopic analyses revealed that the carboxymethyl groups as substituents were also predominantly substituted on the

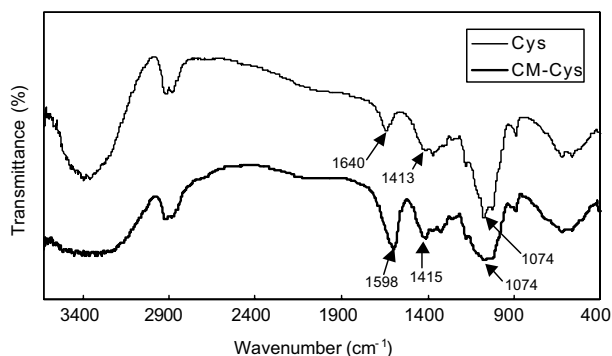
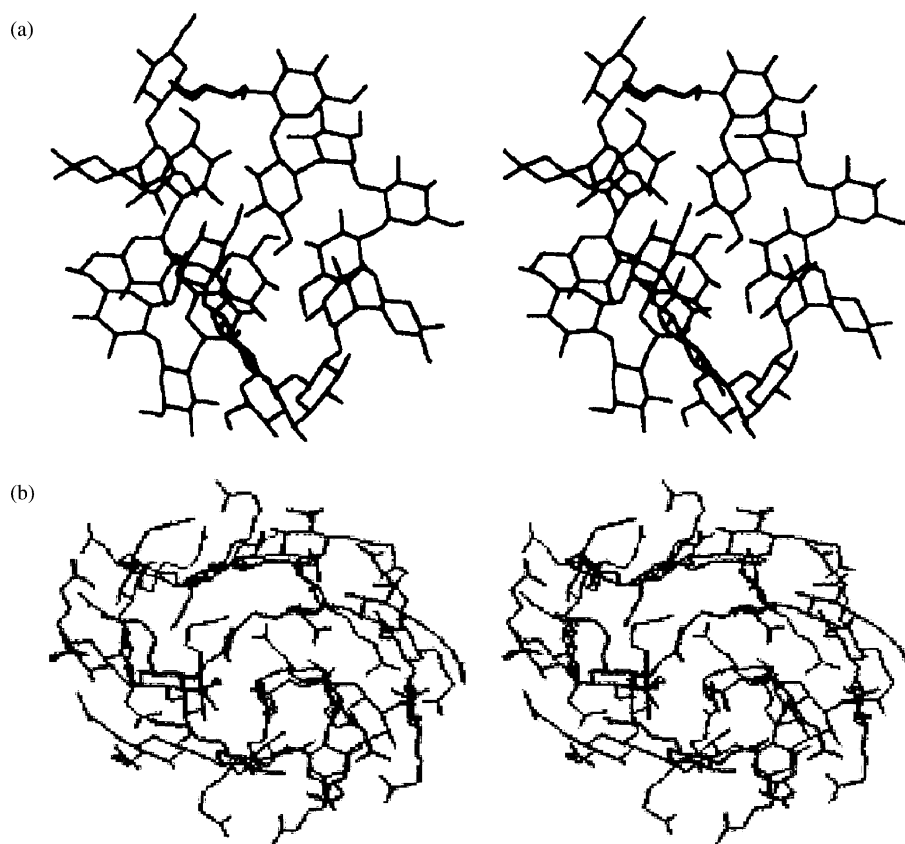


Figure 3. FTIR spectra of native cyclosophoraoses (Cys) (upper trace) and CM-Cys (lower trace). Spectra were acquired between 4000 and 400 cm^{-1} . Bold line: CM-Cys, Normal line: native cyclosophoraoses.

Table 1. Measured and calculated mass units of the m/z peaks of CM-Cys

TNS ^b	DP ^a										
	17	18	19	20	21	22	23	24	25	26	
1	2837 (2812)	3000 (2974)	3163 (3136)	3324 (3298)	3488 (3460)	3649 (3622)	3812 (3784)	3973 (3946)	4135 (4108)	4298 (4270)	
2	2898 (2870)	3058 (3032)	3220 (3194)	3382 (3356)	3544 (3518)	3705 (3680)	3869 (3842)	4031 (4004)	4194 (4166)	4354 (4328)	
3	2953 (2928)	3117 (3090)	3278 (3252)	3441 (3414)	3602 (3576)	3764 (3738)	3926 (3900)	4090 (4062)	4251 (4224)	4412 (4386)	
4	3013 (2986)	3174 (3148)	3336 (3310)	3498 (3472)	3661 (3634)	3823 (3796)	3985 (3958)	4146 (4120)	4309 (4282)	4470 (4444)	
5	3070 (3044)	3232 (3206)	3394 (3368)	3558 (3530)	3720 (3692)	3882 (3854)	4043 (4016)	4205 (4178)	4365 (4340)	4531 (4502)	
6	3128 (3102)	3291 (3264)	3453 (3426)	3616 (3588)	3778 (3750)	3938 (3912)	4101 (4074)	4264 (4236)	4425 (4398)		
7	3185 (3160)	3348 (3322)	3511 (3484)	3673 (3646)	3835 (3808)	3997 (3970)	4160 (4132)	4322 (4294)	4484 (4456)		
8	3242 (3218)	3406 (3380)	3568 (3542)	3732 (3704)	3893 (3866)	4055 (4028)	4218 (4190)	4380 (4352)			
9	3300 (3276)	3462 (3438)	3624 (3600)	3790 (3762)	3950 (3924)	4111 (4086)	4276 (4248)	4438 (4410)			
10	3358 (3334)	3521 (3496)	3683 (3658)	3846 (3820)	4008 (3982)	4170 (4144)	4334 (4306)	4496 (4468)			
11	3415 (3392)	3579 (3554)	3741 (3716)	3902 (3878)	4064 (4040)	4228 (4202)	4392 (4364)				
12	3476 (3450)	3635 (3612)	3799 (3774)	3961 (3936)	4123 (4098)	4285 (4260)	4451 (4422)				
13	3532 (3508)	3696 (3670)	3856 (3832)	4020 (3994)	4183 (4156)	4346 (4318)	4507 (4480)				
14	3590 (3566)	3752 (3728)	3914 (3890)	4078 (4052)	4238 (4214)	4402 (4376)					
15	3649 (3624)	3814 (3786)	3973 (3948)	4135 (4110)	4298 (4272)						

^aDP: degree of polymerization.^bTNS: a total number of substituents. The numbers in parentheses indicate theoretically calculated values.**Figure 4.** Stereoview of molecular models of (a) Cys 21¹⁰ and (b) CM-Cys21.

hydroxyl portions of native cyclosophoraoses at positions 4 and 6. The complexation experiments using CM-Cys as a host molecule showed that the solubility of HB and *N*-AcTrp was enhanced about 5.1-fold and 299-fold in water, respectively. The solubility enhancement of HB and *N*-AcTrp by CM-Cys was explained in the molecular level through ¹H NMR spectroscopic analysis.

3. Experimental

3.1. Bacterial cultures and conditions

R. leguminosarum bv. *trifolii* was used to produce cyclosophoraoses. Precultures were prepared by inoculating the organism into standard GMS media.¹¹ Cells from the late exponential phase were inoculated into 1-L

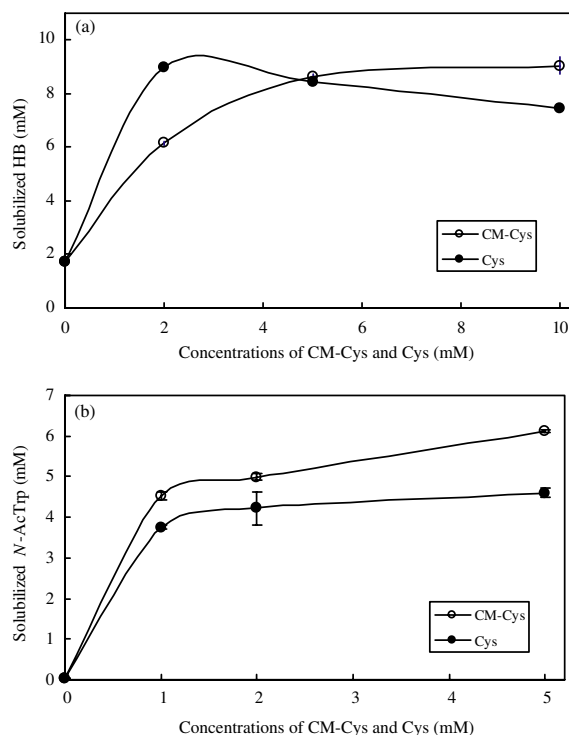


Figure 5. (a) Phase solubility diagrams of HB and (b) *N*-AcTrp complexed with CM-Cys and native cyclophoraoses (Cys). Each point represents the mean \pm standard deviation of three separate experiments.

Erlenmeyer flasks containing 500 mL of $3 \times$ GMS media. The cells were incubated on a rotary shaker (150 rpm) for 12 days at 25 °C and pH 7.0.

3.2. Isolation of cyclophoraoses

After 12 days, extracellular polysaccharides (EPS) and cells in the culture were precipitated by the addition of 3 vol of EtOH. After centrifugation (8000 rpm, 10 min), the 75% alcoholic supernatant was concentrated by rotatory evaporation under vacuum to about 1/10 of the original volume. Up to 8 vol of EtOH was then added to the remaining solution. While this solution stood overnight at 4 °C, a white precipitate of cyclophoraoses was formed and collected by centrifugation (8000 rpm, 10 min). The precipitate was resuspended in water and poured onto a charcoal column. After washing the column with water, adsorbed cyclophoraoses were desorbed with 30% EtOH. This solution was concentrated and then resuspended in 2 mL of 5:5:4 EtOH–BuOH–H₂O. The sample was loaded onto a flash column^{7f} packed with Silica Gel 60 (4 \times 40 cm, 400–230 mesh, E. Merck) and eluted with the same solvent using air pressure to maintain a 1.5 mL/min flow rate. The total elution time of the rhizobial cyclophoraoses was very short, and full separation was completed within 20–30 min. The eluate was collected in 2-mL fractions. The fractions containing cyclophoraoses were desalted on

a column (2 \times 27 cm) packed with Sephadex G-10. The fractions were also confirmed on TLC (E. Merck), and by NMR spectroscopy.

3.3. Preparation of CM-Cys from neutral cyclophoraoses

CM-Cys was prepared based on the previously reported method.¹² A mixture of isolated neutral cyclophoraoses (500 mg) and NaOH (2.8 g) in H₂O (7.4 mL) was added in 16.3% ClCH₂COOH solution (8.1 mL). After being stirred for 4 h at 50 °C, the mixture was adjusted to neutral pH with 6 M HCl. The mixture was then precipitated by adding 5 vol of MeOH and allowed to stand overnight at 4 °C. After centrifugation, the precipitate was resuspended in H₂O and concentrated. Finally, the solution was desalted on a column (2 \times 27 cm) of Sephadex G-10. The modification reaction was monitored on TLC using 5:5:4, EtOH–BuOH–H₂O as a solvent system. For NMR, FTIR, and MALDI MS analyses of CM-Cys, see part 2.2 in the Results and discussion section.

3.4. NMR spectroscopic analysis

NMR spectroscopic analysis was performed on a Bruker AMX spectrometer (operated at 500 MHz for ¹H, 125 MHz for ¹³C) at 25 °C. The purified CM-Cys was dissolved in deuterated water (D₂O, 99.96%). All NMR measurements were performed with 0.7-mL samples in 5-mm NMR tubes. The ¹H and ¹³C signals of CM-Cys were assigned with the combined analysis of a hetero single-quantum coherence (HSQC) spectrum that was obtained at a base frequency of 125 MHz for ¹³C and 500 MHz for ¹H nuclei, ¹H–¹H correlation spectroscopy (COSY) and heteronuclear multiple-bond correlation (HMBC) spectral data. A ¹³C NMR distortionless enhancement polarization transfer (DEPT) spectrum was also obtained at $\theta_z = 135^\circ$ where –CH and –CH₃ signals appeared in the positive phase, with –CH₂ in the negative phase. Chemical shifts are reported relative to a trace of internal sodium 4,4-dimethyl-4-silapentane-1-sulfonate (DSS) at 0.000 ppm, with an accuracy of ± 0.002 ppm.

3.5. FTIR spectroscopic analysis

Fourier-transform infrared spectra were obtained on a JASCO FTIR-300E spectrometer (REV, USA). CM-Cys and neutral cyclophoraoses were dried under vacuum for 1 h and the 1.5–2.0 mg of the purified samples was mixed with a KBr pellet.

3.6. MALDI-TOF mass spectrometry

Mass spectra of CM-Cys were obtained with MALDI-TOF mass spectrometer (Voyager-DETM STR Bio-Spectrometry, Applied Biosystems, Framingham, MA,

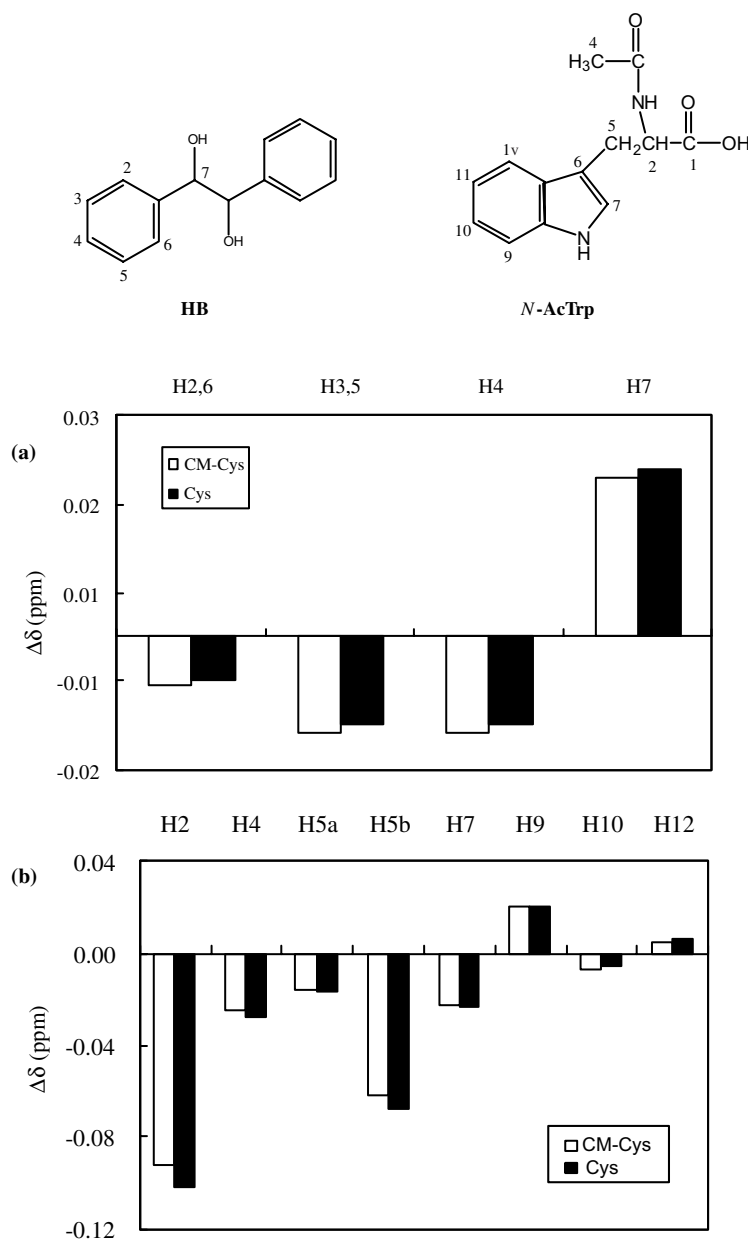


Figure 6. ^1H chemical shift data of CM-Cys, native cyclodextrins (Cys), HB, and *N*-AcTrp, upon the complexation: (a) ^1H chemical shifts of HB and (b) *N*-AcTrp complexed with CM-Cys or Cys, (c) ^1H chemical shifts of CM-Cys and (d) Cys complexed with HB or *N*-AcTrp.

USA) in the positive ion mode using 2,5-dihydroxybenzoic acid (DHB) as the matrix. Approximately 0.5 μL of the sample/matrix mixture was applied to the MALDI probe, and the solvent was removed by evaporation.

3.7. Preparation of inclusion complexes of HB and *N*-AcTrp with the cyclodextrins

CM-Cys and native cyclodextrins were used as host molecules for inclusion complexation. Both HB and *N*-AcTrp were used as guest molecules. First, guest

molecules were dissolved in MeOH to obtain 10 mM of stock solutions. The stock solution (1 mL) was added to the aq host solution (1 mL) with various concentrations. The mixture was stirred for 24 h at room temperature in the dark. After 24 h, the mixture was partially evaporated, lyophilized and dissolved in H_2O (1 mL) to remove uncomplexed guest molecules by filtration using a 0.2- μm membrane filter (Whatman BioScience, UK). The filtrates were lyophilized and dissolved in a mobile phase for HPLC analysis. The concentration of guest molecules in the solution was then quantitatively determined by HPLC.

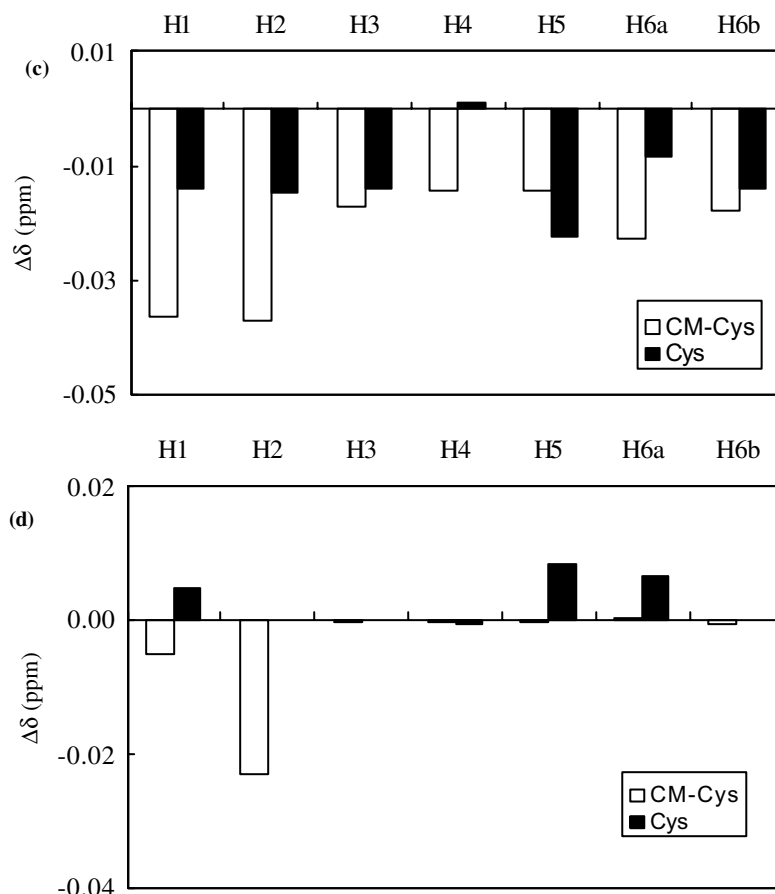


Figure 6 (continued)

3.8. Phase solubility study

Bondclone C_{18} column (10 μ , 300 \times 3.90 mm) was used for HPLC (Shimadzu, Japan) experiments. The analysis was carried out at 30 °C and a flow rate of 0.8 mL/min with 60:40 MeOH–H₂O as the mobile phase. Elution was monitored at 257 nm for HB and at 280 nm for *N*-AcTrp, respectively.

3.9. Computational calculations

CM-Cys21 was built using a CHARMM 28b2 program¹⁸ with a parm22 all-atom force field. Initial coordinates were determined using the SA-MD where the temperature was changed between 300 and 1000 K 60 times continuously. Ten structures were saved at the end of each production phase at 300 K.¹⁰ Total MD simulation time was 3000 ps. After the SA-MD, CM-Cys21 was solvated with a sphere of 27 Å radius of TIP3P water molecules (~2466 water molecules). The solvated CM-Cys21 was energy minimized, and then MD simulations were performed under the constant NVT ensemble for 3000 ps. The temperature was maintained using the Berendsen method ($T = 298$ K,

$\tau = 0.2$ ps). Averaged radius of gyration (R_G) value during MD simulations was estimated from the trajectory file.

Acknowledgements

This research was supported by the National R&D Project for Nano Science and Technology (M1-0214-00-0277) in South Korea SDG.

References

1. Breedveld, M. W.; Miller, K. J. *Microbiol. Rev.* **1994**, *58*, 145–161.
2. Miller, K. J.; Kennedy, E. P.; Reinhold, V. N. *Science* **1986**, *231*, 48–51.
3. Breedveld, M. W.; Miller, K. J. *Microbiology* **1995**, *141*, 583–588.
4. Stanfield, S. W.; Ielpi, L.; O'Brochta, D.; Helinski, D. R.; Ditta, G. S. *J. Bacteriol.* **1988**, *170*, 3523–3530.
5. Spink, H. P. *Plant Mol. Biol.* **1992**, *6*, 977–986.
6. Koizumi, K.; Okada, Y.; Horiyama, S.; Utamura, T.; Higashiura, T.; Ikeda, M. *J. Incl. Phenom.* **1984**, *2*, 891–899.

7. (a) Kwon, C.; Choi, Y.; Kim, N.; Yoo, J.; Yang, C.; Kim, H.; Jung, S. *J. Incl. Phenom.* **2000**, *36*, 55–65; (b) Lee, S.; Kwon, C.; Choi, Y.; Seo, D.; Kim, H.; Jung, S. *J. Microbiol. Biotechnol.* **2001**, *11*, 463–468; (c) Lee, S.; Seo, D.; Kim, H.; Jung, S. *Carbohydr. Res.* **2001**, *334*, 119–126; (d) Lee, S.; Seo, D.; Park, H.; Choi, Y.; Jung, S. *Anton. Leeuw.* **2003**, *84*, 201–207; (e) Seo, D.; Lee, S.; Park, H.; Yi, D.; Ji, E.; Shin, D.; Jung, S. *Bull. Korean Chem. Soc.* **2002**, *23*, 899–902; (f) Seo, D.; Lee, S.; Park, H.; Kwon, T.; Jung, S. *J. Microbiol. Biotechnol.* **2002**, *12*, 522–525.
8. (a) Lee, S.; Jung, S. *Carbohydr. Res.* **2002**, *337*, 1785–1789; (b) Lee, S.; Jung, S. *Carbohydr. Res.* **2003**, *338*, 1143–1146.
9. Mimura, M.; Kitamura, S.; Gotoh, S.; Takeo, K.; Urakawa, H.; Kajiwar, K. *Carbohydr. Res.* **1996**, *289*, 25–37.
10. Choi, Y.; Yang, C.; Kim, H.; Jung, S. *Carbohydr. Res.* **2000**, *326*, 227–234.
11. Breedveld, M. W.; Zenvenhuizen, L. P. T. M.; Zehnder, A. J. B. *Appl. Environ. Microbiol.* **1990**, *56*, 2080–2086.
12. Satomura, S.; Omichi, K.; Ikenaka, T. *Carbohydr. Res.* **1988**, *180*, 137–146.
13. Yang, J.; Du, Y. *Carbohydr. Polym.* **2003**, *52*, 405–410.
14. Riccardo, A. A.; Muzarelli, V. R.; Vesna, S.; Bruno, D.; Monica, M.; Giorgio, T.; Roberto, G. *Carbohydr. Polym.* **1998**, *36*, 267–276.
15. Schiller, J.; Arnhold, J.; Benard, S.; Reichl, S.; Arnold, K. *Carbohydr. Res.* **1999**, *318*, 116–122.
16. Higuchi, T.; Connors, K. A. *Adv. Anal. Chem. Instr.* **1965**, *4*, 117–212.
17. Veiga, F.; Teixeira-Dias, J. J. C.; Kedzierewicz, F.; Sousa, A.; Maincent, P. *Int. J. Pharm.* **1996**, *129*, 63–71.
18. Brooks, B. R.; Bruccoleri, R. E.; Olafson, B. D.; States, D. J.; Swaminathan, S.; Karplus, M. CHARMM: A Program for Macromolecular Energy, Minimization, and Dynamics Calculations. *J. Comput. Chem.* **1983**, *4*, 187–217.